

Index of refraction changes under magnetic field observed in $La_{0.66}Sr_{0.33}MnO_3$ correlated to the magnetorefractive effect

SCOTT M. STRUTNER,^{1,*} ADAM GARCIA,¹ SABINA ULA,¹ CAROLINA ADAMO,² W. LANCE RICHARDS,³ KANG WANG,⁴ DARRELL G. SCHLOM,^{2,5} AND GREG P. CARMAN¹

¹Department of Mechanical and Aerospace Engineering, University of California, Los Angeles, Los Angeles, CA 90095 USA

²Department of Materials Science and Engineering, Cornell University, Ithaca, NY 14853 USA

³NASA Armstrong Flight Research Center, Edwards, CA 93523 USA

⁴Department of Electrical Engineering, University of California, Los Angeles, Los Angeles, CA 90095 USA

⁵Kavli Institute at Cornell for Nanoscale Science, Cornell University, Ithaca, NY 14853 USA

*sstrutner@gmail.com

Abstract: The magnetorefractive effect is a change in a sample's reflectivity with applied magnetic field. This is caused by the material's index of refraction's sensitivity to magnetic fields. However, measurements of the index of refraction as a function of applied magnetic field have not been previously published. This experimental study measures both the magnetorefractive effect and the index of refraction as a function of applied magnetic field and temperature in a 70 nm thick film of lanthanum strontium manganite $La_{0.66}Sr_{0.33}MnO_3$. Index of refraction characterizations were performed with 633 nm light in magnetic fields ranging from -3 kOe to 3 kOe and near the Curie point, at temperatures from 278 K to 308 K.

© 2017 Optical Society of America

OCIS codes: (290.3030) Index measurements; (240.0240) Optics at surfaces; (160.3820) Magneto-optical materials; (160.6840) Thermo-optical materials.

References and links

1. J. Jacquet and T. Valet, "A new magneto-optical effect discovered on magnetic multilayers: the magnetorefractive effect," in *Mater. Res. Symp. Proc.* **384**, 477–490 (1995).
2. S. G. Kaplan, M. Quijada, H. D. Drew, D. B. Tanner, G. C. Xiong, R. Ramesh, C. Kwon, and T. Venkatesan, "Optical Evidence for the Dynamic Jahn-Teller Effect in $Nd_{0.7}Sr_{0.3}MnO_3$," *Phys. Rev. Lett.* **77**, 2081–2084 (1996).
3. D. Hrabovský, J. M. Caicedo, G. Herranz, I. C. Infante, F. Sánchez, and J. Fontcuberta, "Jahn-Teller contribution to the magneto-optical effect in thin-film ferromagnetic manganites," *Phys. Rev. B* **79**, 052401 (2009).
4. Y. P. Sukhorukov, A. V. Telegin, A. B. Granovsky, E. A. Ganshina, A. Zhukov, J. Gonzalez, G. Herranz, J. M. Caicedo, A. N. Yurasov, V. D. Bessonov, A. R. Kaul, O. Y. Gorbenko, and I. E. Korsakov, "Magnetorefractive effect in manganites with a colossal magnetoresistance in the visible spectral region," *J. Exp. Theor. Phys.* **114**, 141–149 (2012).
5. A. B. Granovsky, Y. P. Sukhorukov, E. Gan, and A. V. Telegin, "Magnetorefractive Effect in Magnetoresistive Materials," in *Magnetophotonics: From Theory to Applications*, M. Inoue, M. Levy, and A. V. Baryshev, eds., Springer Series in Materials Science (Springer Berlin Heidelberg, 2013), **178**, pp. 107–133.
6. N. N. Loshkareva, Y. P. Sukhorukov, B. a. Gizhevskii, A. A. Samokhvalov, V. E. Arkhipov, V. E. Naish, S. G. Karabashev, and Y. M. Mukovskii, "Red Shift of Absorption Edge and Nonmetal-Metal Transition in Single Crystals $La_{1-x}Sr_xMnO_3$ ($x = 0.1, 0.2, 0.3$)," *Phys. Status Solidi* **164**, 863–867 (1997).
7. Y. P. Sukhorukov, E. A. Ganshina, B. I. Belevtsev, N. N. Loshkareva, a. N. Vinogradov, K. D. D. Rathnayaka, a. Parasiris, and D. G. Naugle, "Giant change in infrared light transmission in $La_{0.67}Ca_{0.33}MnO_3$ film near the Curie temperature," *J. Appl. Phys.* **91**, 4403 (2002).
8. Y. P. Sukhorukov, a. P. Nosov, N. N. Loshkareva, E. V. Mostovshchikova, A. V. Telegin, E. Favre-Nicolin, and L. Ranno, "The influence of magnetic and electronic inhomogeneities on magnetotransmission and magnetoresistance of $La_{0.67}Sr_{0.33}MnO_3$ films," *J. Appl. Phys.* **97**, 103710 (2005).
9. C. Adamo, X. Ke, H. Q. Wang, H. L. Xin, T. Heeg, M. E. Hawley, W. Zander, J. Schubert, P. Schiffer, D. a. Muller, L. Maritato, and D. G. Schlom, "Effect of biaxial strain on the electrical and magnetic properties of (001) $La_{0.7}Sr_{0.3}MnO_3$ thin films," *Appl. Phys. Lett.* **95**, 112504 (2009).

10. J. F. Ding, O. I. Lebedev, S. Turner, Y. F. Tian, W. J. Hu, J. W. Seo, C. Panagopoulos, W. Prellier, G. Van Tendeloo, and T. Wu, "Interfacial spin glass state and exchange bias in manganite bilayers with competing magnetic orders," *Phys. Rev. B* **87**, 054428 (2013).
11. D. Hrabovský, G. Herranz, K. Postava, I. C. Infante, F. Sánchez, and J. Fontcuberta, "Optical sensing of magnetic field based on magnetorefractive effect in manganites," in *Proc. SPIE* **7356**, 73560R–73560R-10.
12. J. M. C. Roque, "Magneto-Optical Spectroscopy of Complex Systems: Magnetic Oxides and Photonic Crystals," *Universitat Autònoma de Barcelona* (2012).
13. A. B. Granovsky, M. Inoue, and J. P. Clerc, "Magnetorefractive effect in nanocomposites: Dependence on the angle of incidence and on light polarization," *Phys. Solid State* **46**, 498–501 (2004).
14. A. Crook, "The reflection and transmission of light by any system of parallel isotropic films," *J. Opt. Soc. Am.* **38**, 954–964 (1948).
15. H. L. Liu, K. S. Lu, M. X. Kuo, L. Uba, S. Uba, L. M. Wang, and H.-T. Jeng, "Magneto-optical properties of $\text{La}_{0.7}\text{Sr}_{0.3}\text{MnO}_3$ thin films with perpendicular magnetic anisotropy," *J. Appl. Phys.* **99**, 043908 (2006).
16. H. Hosoda, H. Mori, N. Sogoshi, A. Nagasawa, and S. Nakabayashi, "Refractive Indices of Water and Aqueous Electrolyte Solutions under High Magnetic Fields," *J. Phys. Chem. A* **108**, 1461–1464 (2004).
17. W. Prellier, P. Lecoeur, and B. Mercey, "Colossal-magnetoresistive manganite thin films," *J. Phys. Condens. Matter* **13**, R915–R944 (2001).
18. I. J. G. Sparrow, P. G. R. Smith, G. D. Emmerson, S. P. Watts, and C. Riziotis, "Planar Bragg Grating Sensors - Fabrication and Applications: A Review," *J. Sensors*, **2009**, 1-12 (2009).

1. Introduction

Magneto-optics represents the study of the interaction of light with magnetic fields in materials. In 1995, Jacquet and Valet found that the reflectivity and absorptivity of infrared light ($2\ \mu\text{m}$) in magnetoresistive materials are influenced by an applied magnetic field [1] at room temperature. This magnetorefractive effect (MRE) was attributed to conductivity changes influencing the index of refraction in the presence of a magnetic field (i.e., through the Drude-Lorentz model), though the latter was not specifically measured. Subsequent research focused on magneto-transmission (MT) of magnetoresistive materials at shorter wavelengths in the visible spectrum [2]. MT is a change in transmitted light under application of magnetic field. This may be due to a change in the light reflected, as well as a change in the amount of light absorbed during transmission. Additional MRE experiments followed [3] using light in the visible spectrum [4]. While there is general agreement that changes in resistance influence index of refraction in the longer infrared spectrum, there is disagreement [5] as to why the index changes also appear in the shorter visible spectrum, where magnetoresistance does not influence the index of refraction. While several papers have indicated that applied magnetic fields change the index of refraction [1–5], quantitative studies which state the index of refraction changes driving the MRE or MT effects in the visible spectrum have not been published. Papers addressing MRE and MT do not publish sufficient ancillary data to characterize the index of refraction change. Papers have omitted other angle measurements, clear dielectric properties, or multiple angle's reflectivity data. In the course of this work, it was found that this experiment too would not be able to rigorously measure separate index of refraction and extinction coefficients. The lead author was remiss in taking only single polarization measurements. Thus this work reports the index of refraction of LSMO as if the extinction coefficient k is assumed as 0 in the visible spectrum. This is a gross simplification, as the visible spectrum is a region of very high absorption. A rigorous characterizing of the index of refraction and extinction coefficient changes would aid in understanding the physics controlling MRE as well as guide the development of optical devices relying on MRE. This study's weaker characterization hopefully will inspire further study on the topic.

Table 1 provides an overview of MT and MRE studies since the original discovery in 1995. Notably, in 1996, Kaplan et al. [2] measured the MT in the visible spectrum of $\text{Nd}_{1-x}\text{Sr}_x\text{MnO}_3$ ($x = 0.3$) at cryogenic temperatures. Later, Loshkareva et al. [6] studied the MT response of $\text{La}_{1-x}\text{Sr}_x\text{MnO}_3$ ($x = 0.1$) over the $2.5\ \mu\text{m}$ to $11\ \mu\text{m}$ spectral range. In 2002, Sukhorukov et al. [7] demonstrated near room temperature MT in $\text{La}_{1-x}\text{Cr}_x\text{MnO}_3$ ($x = 0.33$) using a $6.4\ \mu\text{m}$ wave-

Table 1. Progression of MRE/MT research in literature.

Year	Material	Effect	Sensitivity (Δ/kOe)	T (K)	λ (μm)	Ref.
1995	$[Ni_{80}Fe_{20}/Cu/Co/Cu]$	MT	1.47	300	9	[1]
1996	$Nd_{1-x}Sr_xMnO_3$ ($x=0.3$)	MT	-2.81 E-3	180	1.37	[2]
1997	$La_{1-x}Sr_xMnO_3$ ($x=0.1$)	MT	1.88 E-2	132	4.85	[6]
2002	$La_{1-x}Ca_xMnO_3$ ($x=0.33$)	MT	-3.38 E-2	273	6.4	[7]
2005	$La_{1-x}Sr_xMnO_3$ ($x=0.33$)	MT	5.88 E-3	356	1.5	[8]
2009	$La_{1-x}Sr_xMnO_3$ ($x=0.33$)	MRE	-3.57 E-5	300	0.650	[3]
2012	$La_{1-x}Ag_xMnO_3$ ($x=0.1$)	MRE	-2.60 E-3	310	0.833	[4]

length source. Progress by Sukhorukov et al. continued, and in 2005 they measured above room temperature MT [8] at common optical wavelengths (i.e., 1550 nm) in $La_{1-x}Sr_xMnO_3$ ($x=0.33$). Sukhorukov et al. [8] further showed the MT effect was linear for fields ranging from 0 kOe to 10 kOe for 5.6 μm wavelengths. Hrabovsky et al. demonstrated the first visible spectrum MRE, showing a 0.025% reflectivity decrease in reflected 633 nm light at 7 kOe for a $La_{1-x}Sr_xMnO_3$ ($x=0.33$) film at room temperature [3]. In 2012, researchers from the Hrabovsky and Sukhorukov groups [4] studied MRE in the visible spectrum (i.e. 300 to 1300 nm) at room temperature in $La_{1-x}Cr_xMnO_3$ ($x=0.3$) and $La_{1-x}Ag_xMnO_3$ ($x=0.1$) samples. While all of these represent significant advancements, none have reported index of refraction measurements, though they are stated to be the source of both MT and MRE [1–5].

In this study, we experimentally measure the reflectivity of $La_{1-x}Sr_xMnO_3$ ($x=0.33$) (LSMO) as a function of angle, magnetic field and temperature. An index of refraction is fitted to the reflectivity as a function of angle, assuming the index is non-complex. This allows index of refraction to be assessed as a function of magnetic field and temperature. To ease discussion of unit-less index of refraction, we shall use the unit-less unit of "refractive index units" (RIU). MRE measurements were made using a 633 nm laser and show a nearly linear decrease in sample reflectivity as a function of field, decreasing by 0.95% at 5.5 kOe at 288 K, which is near the Curie temperature (T_C) of the LSMO film used in this study [9]. Index of refraction also decreased by 4.8×10^{-3} refractive index units (RIU) for an applied 3 kOe field at 290 K or a sensitivity of $-1.6 \text{ mRIU}/\text{kOe}$.

2. Experimental setups

A 70 nm thick film of $La_{1-x}Sr_xMnO_3$ ($x=0.33$) was grown using reactive molecular-beam epitaxy on a 1 mm thick (110) oriented NdGaO₃ substrate with the method described by Adamo et al. [9]. The sample was tested using the two setups, shown in Figs. 1(a) and 1(b), for MRE and index of refraction measurements, respectively. Figure 1(a) shows the fixed angle reflectivity setup's main components [3]. The optical path consists of a laser which shines light through a vertically oriented polarizer, into a cryostat with the sample oriented at 5° with respect to the laser source, and out of the cryostat onto a photodiode. Two lasers of 1550 nm and 633 nm wavelength were used in this study. These MRE tests consist of sweeping a magnetic field from 5.3 kOe to -5.3 kOe then back to 5.3 kOe for three cycles while the sample's reflectivity was measured with a photodiode. The Magnetic field was measured with a Hall effect probe (not shown in Fig. 1(a)) placed behind the cryostat and adjacent to the sample. Tests were conducted at fixed temperatures ranging from 275 K to 305 K using an integrated heater and thermal couple for sample temperature control within the cryostat.

Figure 1(b) shows the test setup to measure the index of refraction. This test setup consists of a 633 nm laser shining light through a polarizer into a test chamber and onto the sample.

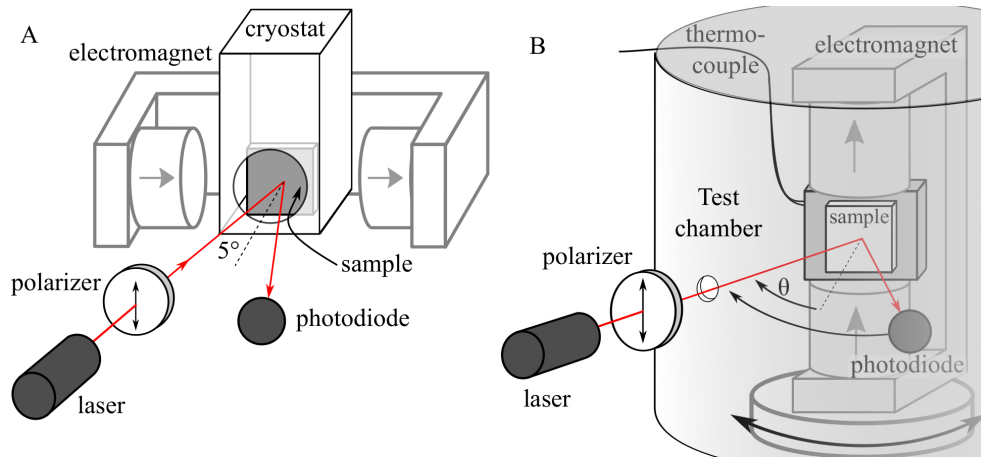


Fig. 1. Experimental setup for A) MRE fixed angle ($\theta < 5$ deg) reflection measurements system. The temperature was controlled via a cryostat, necessitating illumination through a quartz viewing window. B) Index characterizing ellipsometer with heat generated by the electromagnet coils and chilling achieved via a cold air supply flowed into the test chamber.

The light is reflected off the sample and onto a photodiode detector enclosed within the chamber. The sample and electromagnet are mounted onto a rotating stage allowing the angle of incidence of the laser to be varied by θ . The index of refraction test consisted of performing reflection measurements for (θ) values between 66° and 55° in steps of 0.75° . The absolute positioning accuracy relative to 0° is $\pm 1^\circ$, with the stage performing relative positioning to $\pm 0.01^\circ$ between readings and index characterizations. This yields a $\pm 4\%$ uncertainty in base index measurements, but a $\pm 0.04\%$ relative uncertainty or ± 0.8 mRIU. Before and during each index test, the electromagnet applied a constant magnetic field with values ranging -2.9 kOe to 2.9 kOe. The sample's temperature was tracked using a surface mounted thermocouple attached to the sample's aluminum holder.

3. Experimental results

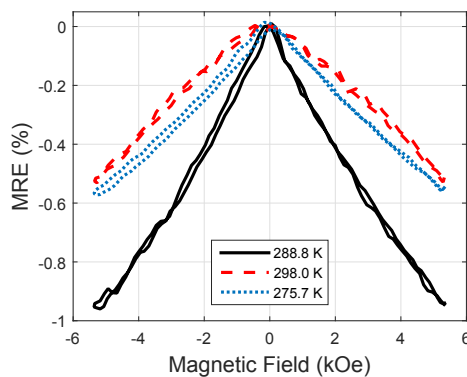


Fig. 2. Reflectivity of 633 nm light vs. magnetic field for the sample at three temperatures, 275.7 K, 288.8 K and 298.0 K.

Figure 2 shows MRE vs. applied field for tests conducted at three temperatures, 275.7 K,

288.8 K and 298.0 K with a 633 nm laser with the Fig. 1(a) test setup. The magnetorefractive effect is defined as

$$MRE(\%) = \frac{R(H) - R(0)}{R(0)} \quad (1)$$

where $R(0)$ is the zero field reflectivity and $R(H)$ is the reflectivity at the measured field [1]. The data shows a negative MRE value, that is reflectivity decreases as the magnetic field increases, for all temperatures measured. The negative reflectivity is due to UV absorption bands shifting as the electronic structure (specifically, the localized electrons) is modified by magnetic fields as explained by the Jahn-Teller interactions [3]. Comparing the data in Fig. 2, the slope is approximately $-0.11\%/kOe$ for the cold reading, 275.7 K which increases to $-0.18\%/kOe$ at 288.8 K and decreases to $-0.10\%/kOe$ at the warm reading, 298.0 K. However, the data taken at 298.0 K shows a slight nonlinear response, i.e., the slope increases as the field increases. We attribute this nonlinearity to the influence of the applied magnetic field on T_C [10], which is approximately 290 K [9], [11]. This MRE data has similar trends to previous reports [3], [12] but with different magnitudes. The differences are attributed to dissimilarities in test setup such as angles of incidence and film thicknesses [13].

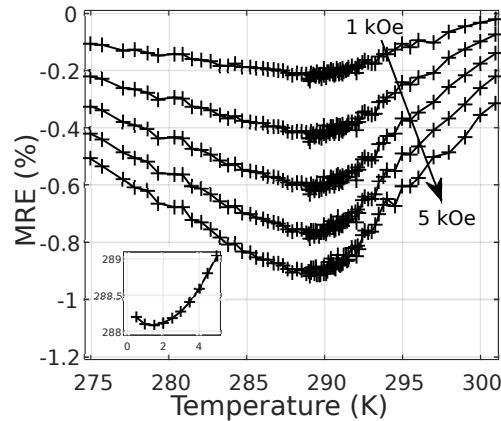


Fig. 3. MRE of 633 nm light vs. temperature for five applied absolute field values. Inset tracks the temperature of maximum MRE, T_M , vs. applied field.

Figure 3 shows MRE test data for 633 nm light as a function of temperature for five applied magnetic fields and the setup in Fig. 1(a). The MRE first increases in absolute magnitude with increasing temperature followed by a decrease after 290 K for all fields studied [3]. The local effect maximums, T_M , observed in the figure at are attributable to the Jahn-Teller interactions directly related to the material's susceptibility. The susceptibility is maximal near T_C of the material and thus produces a maximum shift in the UV absorption bands. The Fig. 3 inset shows a plot of T_M found via polynomial fitting of the local values versus applied field. As one can see, T_M increases as the field increases from 0 kOe to 5.0 kOe. We attribute this to the magnetic field's influence on T_C by stabilizing the spin states to remain ordered [10] at higher temperatures.

Figure 4 shows MRE results as a function of temperature for five applied magnetic fields using a 1550 nm light source and the setup in Fig. 1(a). This test shows positive MRE for all fields and temperatures as contrasted with the negative MRE values reported in Figs. 2 and 3. Also, while the trends are similar, the absolute value of the MRE shown in Fig. 4 is an order of magnitude smaller than that shown in Fig. 3. The reason for both of these (the magnitude decrease and sign inversion) is that there is now a second opposing MRE phenomenon. At longer wavelengths the delocalized electrons' movement i.e. the Drude-Lorentz response, dominates

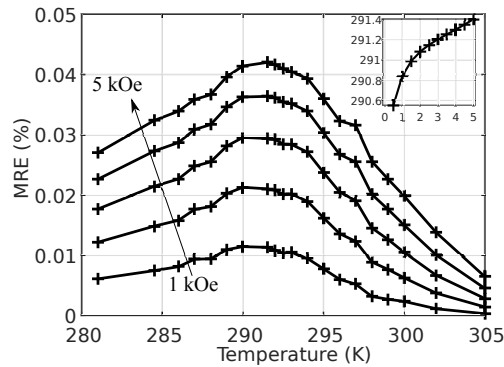


Fig. 4. MRE of 1550 nm light vs. temperature for five applied absolute field values. Inset is the fitted peak MRE vs. temperature.

the material's net response. This effect opposes the localized electrons response i.e. the Jahn-Teller effect. The peak in MRE is caused by the magnetoresistance peaking at T_C . The inset shows that the temperature at which peak MRE occurs (T_M), shifts with the applied magnetic field by a similar magnitude amount as reported in the 633 nm characterization shown in Fig. 3. However, the concavity difference is likely attributed to the Drude-Lorentz effect present in the 1550 nm study but absent in the 633 nm study. As the 633 nm testing showed a stronger net MRE than the 1550 nm testing, 633 nm was used in the second part of this study.

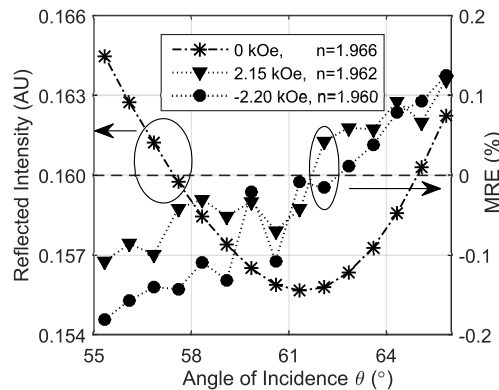


Fig. 5. Reflected Intensity and MRE of 633 nm light vs. angle for three passes at different magnetic field conditions. The reflected intensity for no applied field is plotted using the left axis, and the change in reflectivity with applied field is quantified as MRE for the two applied field conditions and plotted with the right axis.

Figure 5 shows data from tests performed at 289 K using a 633 nm light source with the test setup shown in Fig. 1(b). The data represented with asterisks is the reflected intensity (i.e. left axis) vs. angle without an applied magnetic field. All tests were conducted near the Brewster's angle (61.5°) to improve the index of refraction characterization. The reflected intensity data shows a continuous and smooth reflected intensity vs. angle of incidence relationship. The index of refraction is determined by fitting a mono-film on bulk substrate reflectivity equation [14] to the reflected intensity vs. angle of incidence data using only non-complex indices, with a fixed film thickness of 70 nm and a substrate index of 2.12 RIU. From literature, there is an expectation that the index of refraction in LSMO is complex [15]. The index changes found here are actually split between both the real and imaginary components. This method of ignoring the

extinction coefficient of LSMO finds the fitted index of refraction for the zero field data to be 1.966 RIU. The data represented by triangles and circles in Fig. 5 are the magnetically driven change in reflectivity, the MRE (i.e. right axis) vs. angle for applied magnetic fields of 2.15 kOe and -2.2 kOe, respectively. These MRE values were calculated from the reflected intensity measurements performed vs. the zero field condition for each angle of incidence. The MRE values follow a trend from negative values below the Brewster's angle to positive values above it [13]. All reflectivity changes are attributed to MRE, as there is no polarizer in the reflected light's path. Any polarization rotations from non-linear classical magneto-optical effects will not effect the intensity measurements. The calculated index of refraction is 1.962 RIU at 2.15 kOe while for -2.20 kOe it is 1.960 RIU. Both of these indices with applied magnetic fields are smaller than that measured at 0 Oe.

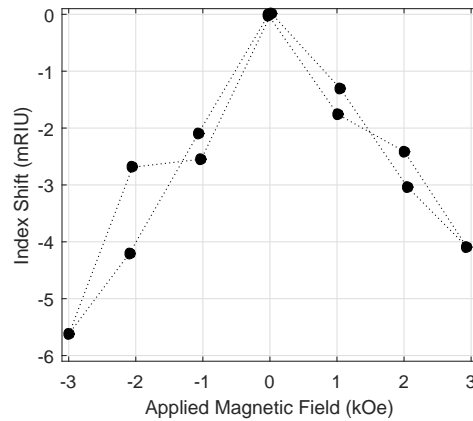


Fig. 6. Index Shift vs. Applied Magnetic Field for 13 characterizations cycled from 0 to -3 to 3 kOe to 0 kOe, with the temperature rising from 288 K to 292 K during the cycle.

Figure 6 shows the index shift as a function of the magnetic field with the index shift normalized to that measured at $H=0$ Oe. These values were determined using a similar approach to that presented in Fig. 5. The Fig. 6 data shows that the index decreases in a linear manner for both positive and negative applied magnetic fields. The average slope in Fig. 6 defines the index of refraction's magnetic sensitivity. This average slope is calculated to be -1.6 mRIU/|kOe| at 290 K and the difference between the positive and negative applied fields is considered minor, and within experimental error.

Figure 7 shows the index of refraction's magnetic sensitivity as a function of temperature. Each point is determined by fitting a slope to index characterization sets as a function of magnetic field for different temperatures, as described in Fig. 6. A Gaussian model defined by

$$\frac{dn}{dH} = \alpha \exp \left[- \left(\frac{T_C - T}{T_s} \right)^2 \right] \quad (2)$$

is fitted to the sensitivity vs. temperature data, finding fitted values for: magneto-optical coefficient $\alpha = -1.6$ mRIU/|kOe|, Currie temperature $T_C = 288.8$ K, and temperature span of the effect $T_s = 10.2$ K. The material's magnetic sensitivity follows a Gaussian profile that initially increases in absolute magnitude up to -1.6 mRIU/|kOe| at T_C and then subsequently decreases to 0 mRIU/|kOe| at 310 K. The MRE of the material (see Fig. 3) also peaks at T_C , reinforcing the assertion that index of refraction dictates MRE changes. The magnitude of LSMO's magneto-optical coefficient α is 120 times larger than and opposite in sign to that of water's, which is 0.013 mRIU/|kOe| [16].

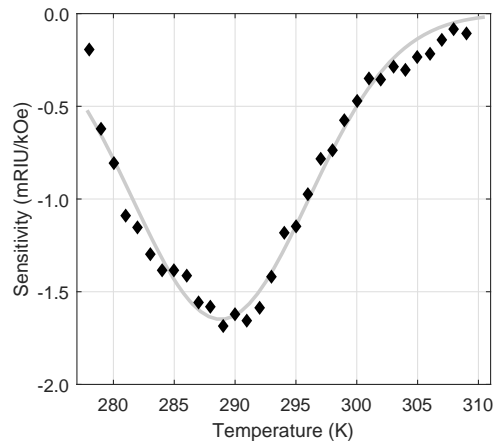


Fig. 7. Sensitivity vs. Temperature, and fitted line using a Gaussian model for sensitivity.

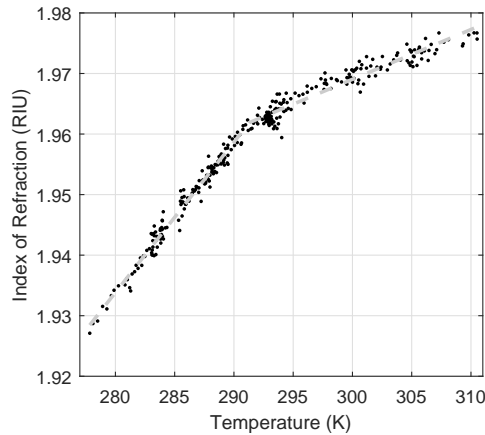


Fig. 8. Index of Refraction vs. Temperature for characterizations performed with $H=0$ kOe.

Figure 8 shows the index of refraction vs. temperature for tests performed at zero magnetic field. The index of refraction increases with temperature and there is a noticeable slope change at 291.3 K, i.e., T_C . This thermo-optical slope change is most likely driven by the reported thermal-resistance slope change T_C [17]. The thermal-resistance change produces a change in the electronic structure which has a direct impact on the index of refraction. Using the data presented in Fig. 8, a linear thermo-optic model is proposed,

$$n = n_C + (T - T_C) \frac{dn}{dT} \quad (3)$$

where n_C is the index of refraction at the Currie temperature and equals 1.962(80) RIU. The slope dn/dT is defined as,

$$\frac{dn}{dT} = \begin{cases} \beta_F & T < T_C \\ \beta_P & T \geq T_C \end{cases} \quad (4)$$

where β_F is the thermo-optic coefficient of the ferromagnetic phase equal to 2.5 mRIU/K, and β_P is the thermo-optic coefficient of the paramagnetic phase equaling 0.8 mRIU/K. As one can see, this model accurately captures the experimental trend observed in the figure.

Using Eqs. (2), (3), and (4), a new phenomenological equation describing the index of refraction as a function of magnetic field and temperature can be introduced:

$$n(H, T) = n_C + |H|\alpha \exp \left[- \left(\frac{T_C - T}{T_s} \right)^2 \right] + (T - T_C) \begin{cases} \beta_F & T < T_C \\ \beta_P & T \geq T_C \end{cases} \quad (5)$$

It is expected that n_C , α , β_F , and β_P , are functionally dependent upon a number of parameters especially the wavelength of light. This work addressed the index of refraction of LSMO as only a real value. Equation (5) provides the community a mathematical representation of the material's optical response to applied magnetic fields and temperatures. This model provides an initial platform to further describe and potentially understand MRE effects in the visible spectrum. For applications utilizing MRE, a rough approximation of device sensitivity may now be estimated. For magnetic field sensing, if all the fitted index shifting reported here was from changes in the real spectrum, then when LSMO is coated onto a tapered planar Bragg grating, of the type made by Sparrow et al. which has a 1.9×10^{-3} mRIU resolution [18], the resulting device would have a $1.2 |\text{Oe}|$ resolution. As α is so much smaller than either β though, such a sensor would be greatly susceptible to even minute thermal fluctuations.

4. Conclusion

This paper describes tests to measure the magnetorefractive effect and the index of refraction as a function of temperature and magnetic field for an LSMO thin film. Results show that both effects are maximum at or near the Curie temperature. The film's response is dependent upon the wavelength of light used, which is explained by UV absorption bands shifting and by the IR affecting Drude-Lorenz resistance changes representing competing effects in the visible spectrum. While the index of refraction changes linearly with temperature, there is a discontinuity near the Curie point, which is attributed to the thermal resistance of the material changing. In addition to experimental results, a phenomenological model is presented for the index of refraction as a function of temperature and magnetic field, to guide the design of future novel magneto-optical devices utilizing MRE. Results also support the previous literature assertions that MRE changes are directly related to index of refraction changes.

Funding

The authors thank the National Aeronautics and Space Administration (NASA) and the Aero Institute for funding this work through PO AERO 661. The authors thank the Translational Applications of Nanoscale Multiferroic Systems (TANMS) Engineering Research Center (ERC) funded by the National Science Foundation (NSF) through Cooperative Agreement Award EEC-1160504 for funding the interns who worked on this project.